Lab on a Chip

PAPER

Cite this: *Lab Chip*, 2024, **24**, 3243

Parathyroid-on-a-chip simulating parathyroid hormone secretion in response to calcium concentration†

Sunghan Lee,‡[ab] Hyo-Il Jung, ‡[ac] Jaehun Lee,[ab] Youngwon Kim,[ab] Jaewoo Chung,[d] Han Su Kim,[e] Jiseok Lim,[fg] Ki Chang Nam,[b] Yun-Sung Lim,*[h] Han Seok Choi*[i] and Bong Seop Kwak *[bg]

Received 20th March 2024,
Accepted 27th May 2024

DOI: 10.1039/d4lc00249k

rsc.li/loc

The parathyroid gland is an endocrine organ that plays a crucial role in regulating calcium levels in blood serum through the secretion of parathyroid hormone (PTH). Hypoparathyroidism is a chronic disease that can occur due to parathyroid defects, but due to the difficulty of creating animal models of this disease or obtaining human normal parathyroid cells, the evaluation of parathyroid functionality for drug development is limited. Although parathyroid-like cells that secrete PTH have recently been reported, their functionality may be overestimated using traditional culture methods that lack *in vivo* similarities, particularly vascularization. To overcome these limitations, we obtained parathyroid organoids from tonsil-derived mesenchymal stem cells (TMSCs) and fabricated a parathyroid-on-a-chip, capable of simulating PTH secretion based on calcium concentration. This chip exhibited differences in PTH secretion according to calcium concentration and secreted PTH within the range of normal serum levels. In addition, branches of organoids, which are difficult to observe in animal models, were observed in this chip. This could serve as a guideline for successful engraftment in implantation therapies in the future.

1. Introduction

The parathyroid glands are a major regulatory organ that maintains serum calcium concentration within the physiological range,[1] and are responsible for detecting low levels of calcium in the serum and secreting PTH. If there is insufficient PTH in the body, hypocalcemia, muscle cramps, or ectopic calcification associated with hypoparathyroidism can occur.[2] Standard treatment for hypoparathyroidism involves taking calcium salts and active vitamin D metabolites,[3] but weekly or bi-weekly monitoring is required during the initial dosage adjustment period.[4] While exogenous calcium and vitamin D analogs can maintain normal serum calcium concentrations, they can lead to progressive renal calcium deposition which eventually progresses to renal failure.[5] Transplantation is an effective approach to treating organ failure, but both allografts and xenografts are susceptible to immunological rejection.[6] Therefore, there is a need for pharmacological treatments that aim to restore parathyroid functionality at a fundamental level to overcome the limitations of current therapies. However, the current pharmaceutical industry is facing the problem of numerous drug candidates being abandoned before reaching the clinical stage.[7] The primary reasons for this problem include the inaccurate determination of drug candidate efficacy due to biological differences between humans and animals, as well as the significant time and cost involved in animal experiments. Furthermore, traditional culture methods for cells or organoids lack similarity to *in vivo* conditions, such as interaction with blood vessels and

[a] *School of Mechanical Engineering, Yonsei University, 50 Yonsei-ro, Seadaemun-gu, Seoul, 13722, Republic of Korea*
[b] *College of Medicine, Dongguk University, 32 Dongguk-ro, Ilsandong-gu, Goyangsi, Gyeonggi-do, 10326, Republic of Korea. E-mail: bskwak82@gmail.com; Tel: +82 31 961 5803, +82 10 4477 3865*
[c] *The DABOM Inc., 50 Yonsei-ro, Seodaemun-gu, Seoul, 03722, Republic of Korea*
[d] *Department of Laboratory Medicine, Dongguk University Ilsan Hospital, 27 Dongguk-ro, Ilsandong-gu, Goyang-si, Gyeonggi-do 10326, Republic of Korea*
[e] *Department of Otorhinolaryngology-Head & Neck Surgery, Ewha Womans University, School of Medicine, Seoul 158-710, Republic of Korea*
[f] *School of Mechanical Engineering, Yeungnam University, 280 Daehak-ro, Gyeongsan-si, Gyeongsangbuk-do, 38541, Republic of Korea*
[g] *MediSphere Inc., 280, Daehak-ro, Gyeongsan-si, Gyeongsangbuk-do, 38541, Republic of Korea*
[h] *Department of Otorhinolaryngology -Head and Neck Surgery, Dongguk University Ilsan Hospital, 27 Dongguk-ro, Ilsandong-gu, Goyang-si, Gyeonggi-do 10326, Republic of Korea. E-mail: splash1@hanmail.net; Tel: +82 10 2965 8318*
[i] *Department of Internal Medicine, Division of Endocrinology and Metabolism, Dongguk University Ilsan Hospital, 27 Dongguk-ro, Ilsandong-gu, Goyang-si, Gyeonggi-do 10326, Republic of Korea. E-mail: hschoi402@dumc.or.kr; Tel: +82 10 8631 4747*

† Electronic supplementary information (ESI) available. See DOI: https://doi.org/10.1039/d4lc00249k

‡ These authors contributed equally to this paper.

the extracellular matrix (ECM), which can lead to a misassessment of their functionality. This discrepancy arises because the endocrine system, including the parathyroid gland, indeed closely interacts with blood vessels to regulate various bodily functions and processes.[8] Additionally, direct communication with the culture medium may not appropriately reproduce *in vivo* conditions.

One of the attempts to resolve the limitations of animal experiments and traditional culture methods is organ-on-a-chip technology. Organ-on-a-chip, which are *in vitro* systems capable of bridging the gap between traditional cell cultures and animal models or human subjects, are being developed as a complementary approach to animal experiments.[9–11] Several organ-on-a-chip, such as heart-on-a-chip,[12] lung-on-a-chip,[13] liver-on-a-chip,[14] gut-on-a-chip,[15] and kidney-on-a-chip,[16] have been developed. While the lack of reliable animal models and cell lines for parathyroid research highlights the urgent need for an *in vitro* tool that can simulate the function of the parathyroid gland, there is currently an absence of a parathyroid-on-a-chip. In this study, parathyroid organoids were fabricated from tonsil-derived mesenchymal stem cells (TMSCs) using the droplet-based microfluidics system, which facilitates mass fabrication with uniform size of organoids. Then, we developed parathyroid-on-a-chip, which can simulate PTH secretion based on calcium concentrations. This chip can serve as a complementary tool to animal models for the development of drugs for parathyroid disease, reducing the cost and time of new drug development.

2. Materials and methods

2.1 TMSC isolation and culture

Tonsil tissues were obtained from donors aged 5 to 15 years who underwent tonsillectomy, with informed consent obtained from the participants and approved by Dongguk University Ilsan Hospital Institutional Review Board (IRB file no. 2022-12-028). TMSCs were isolated and cultured using the well-established protocol.[17–20] Tonsil tissues were chopped and digested in Dulbecco's Modified Eagle Medium with high glucose (DMEM-HG, WelGENE Inc., Daegu, Korea) containing 205 U mL^{-1} collagenase type I and 10 μg mL^{-1} DNase for 30 min at 37 °C. Digested tissues were filtered by a mesh for removing debris, and cells were collected by centrifugation at 1300 rpm for 3 min. The cells were washed twice in DMEM-HG with 20% fetal bovine serum (FBS) and once more in DMEM-HG with 10% FBS. Mononuclear cells were obtained by Ficoll-Paque density gradient centrifugation and filtered with a 70 μm strainer. They were then washed once in DMEM-HG with 10% FBS, 100 μg mL^{-1} streptomycin, and 100 U mL^{-1} penicillin. Obtained cells were seeded at a density of 1×10^8 cells per T-175 culture flask in DMEM-HG with 10% FBS, 100 μg mL^{-1} streptomycin, and 100 U mL^{-1} penicillin. After 48 hours, the medium was changed, and non-adherent cells and residual blood cells were removed. Remaining adherent mononuclear cells which are called TMSCs were cultured for 2–3 weeks for over 90% confluency. The culture medium was changed twice a week. All TMSCs used in this study were passage between 3–7.

2.2 Identification of cell subtype

TMCSs or parathyroid-like cells were stained with negative and positive stem cell markers to define primitive stem cell identity. The cells were each prepared at 1×10^5 cells ml^{-1} in a round bottom-type microtube. Cells were washed twice in 4 °C stain buffer (BD Science, San Diego, CA), and added each cell marker antibodies. Cells were reacted for 30 min at 4 °C and washed twice in stain buffer. Negative stem cell markers were hematopoietic cell antibodies; PE-CD34, FITC-CD45, PE-CD14, and endothelial antibodies; PE-CD31 (BD Science, San Diego, CA). Positive stem cell markers were primitive stem cell antibodies; PE-CD73, FITC- CD90, and FITC-CD105 (BD Science, San Diego, CA). Non-stained cells were also measured by using a control. Stained cells were analyzed by a flow cytometry system (Novocyte 2000R, ACEA Biosciences, USA).

2.3 Immunofluorescence and cytoskeleton staining

Parathyroid-like cells and parathyroid organoids were fixed using a 4% paraformaldehyde (Sigma-Aldrich, MO) solution for 30 minutes, and then were blocked and permeabilized with a solution containing 2% bovine serum albumin and 0.1% Triton X-100 (Sigma-Aldrich, MO). They were incubated overnight at 4 °C with PTH antibody (1 : 100, PAA866Ra01, Cloud-clone Corp, Houston, TX) and CaSR antibody (1 : 100, ab19347, Abcam, Cambridge, MA). After the primary antibody binding, the secondary antibodies for PTH (1 : 200, ab150077, Abcam, Cambridge, MA) and CaSR (1 : 100, ab150118, Abcam, Cambridge, MA) were applied for 4 hours at room temperature. For visualizing purposes, TMSC cytoskeleton staining was performed following the protocol described above for fixation, blocking, and permeabilization. TMSCs were then stained using 5 units ml^{-1} of Alexa Fluor™ 488 Phalloidin (A12379, Thermo Fisher Scientific, Cleveland, OH) for 3 hours at room temperature. To visualize the cell nuclei, DAPI was used as a counterstain.

2.4 Formation of TMSC organoids

Formation of organoids was conducted at MediSphere Inc. (Gyeongsangbuk-do, Republic of Korea). Briefly, TMSC organoids were formed using a droplet-based microfluidic system. This system allows mass-producing organoids (or spheroids) by rapidly generating cells encapsulated in droplets. It enables the fabrication of organoids of precisely targeted size by controlling the number of cells encapsulated in each droplet.[21] We prepared TMSCs at a concentration of 5×10^6 cells ml^{-1} (3 ml) and injected them into the aqueous phase inlet of the droplet-based microfluidic system, while 5% surfactant (FluoSurf-C™, Emulseo, France) HFE-7500 oil (3MTM, MN, USA) was injected into the oil phase, as shown in Fig. S1.† Both solutions were simultaneously

injected at flow rates of 60 μl min^{-1} and 150 μl min^{-1}, respectively, using syringe pumps (NE-4000, New Era Syringe Pumps). During the injection, we operated the syringe pump vertically to minimize uneven cell counts caused by cell sedimentation.

Prepared TMSCs at a concentration of 5×10^6 cells ml^{-1} were encapsulated within droplets, each containing an average of 166 ± 5 cells $droplet^{-1}$. Subsequently, these droplets were incubated for 24 hours to allow the formation of TMSC organoids. TMSC organoids were collected from the droplets using 1*H*,1*H*,2*H*,2*H*-perfluoro-1-octanol (Sigma-Aldrich, MO) as a droplet-releasing reagent.

2.5 Differentiation into the parathyroid phenotype

TMSCs were differentiated into parathyroid-like cells using the modified Bingham protocol,[22] as a well-established protocol.[17–20] TMSCs were incubated in DMEM-HG for over 90% confluency on a 2D culture dish, and then they were cultured with a differentiation medium containing 100 ng ml^{-1} activin A and 100 ng ml^{-1} soluble sonic hedgehog (Shh) for 7 days. The differentiation medium was changed every other day during the differentiation period. TMSCs that undergo differentiation for 7 days are called parathyroid-like cells.

To obtain parathyroid organoids, we opted to initially fabricate TMSC organoids and subsequently differentiate them into parathyroid phenotypes because the TMSC organoid state indicates higher cell survival rates and levels of PTH expression compared to parathyroid organoids derived directly from differentiated cells.[18] TMSC organoids were transferred to an ultra-low attachment surface well plate (Corning Inc., Corning, NY) to reduce the merging between organoids and maintain their 3D morphology. Subsequently, they were cultured for 7 days in a culture medium containing differentiation factors, following a differentiation process similar to TMSCs. Organoids that undergo differentiation for 7 days are called parathyroid organoids.

2.6 Fabrication of parathyroid-on-a-chip

The parathyroid-on-a-chip consists of two channels, one for the blood vessel and the other for the parathyroid microenvironment, as shown in Fig. S2.† The width of the blood vessel and parathyroid channels is 1000 μm and 800 μm, respectively, and the depth of both channels is 200 μm. The five equilateral triangular posts with a length of 350 μm are arranged to separate the two channels. The gaps between the posts are 100 μm, which is designed so that the gaps have the largest size (100 μm) within the commonly used range,[23–26] because larger gaps are advantageous for smooth interaction between the two channels. The parathyroid-on-a-chip was fabricated with polydimethylsiloxane (PDMS, Corning Inc., Corning, NY) replica molding and was formed on a patterned SU-8 silicon wafer. The PDMS replica was perforated for the inlet and outlet and was bonded on a glass substrate using an oxygen plasma treater (Electro-Technic Products, Chicago, IL).

For the formation of the parathyroid microenvironment, 200 parathyroid organoids suspended in 5 μl of DMEM-HG, 1 μl of thrombin solution (10 units ml^{-1}) and 4 μl of fibrinogen solution (10 mg ml^{-1}) were added and mixed quickly. The parathyroid microenvironment channel was filled with the parathyroid organoid-laden fibrin gel. Then, the blood vessel channel was coated with 0.1 mg ml^{-1} concentration of fibronectin at 37 °C for 60 min. 2×10^5 human umbilical vein endothelial cells (HUVECs) in 40 μl of EBM-2 (Endothelial Cell Growth Basal Medium-2, Lonza, Walkersville, MD) were injected into the blood vessel channel and incubated for 40 min vertically for the formation of vascular endothelium. After returning to the original position, 200 μl of DMEM-HG with different calcium concentrations, including low (0.3 mM), normal (1.8 mM), and high (3.3 mM) $CaCl_2$, was added to the blood vessel channel individually, and incubated at 37 °C in 5% CO_2. The culture medium was changed and collected every 48 hours, and the last culture medium on day 6 was changed with a medium containing a normal calcium concentration under all conditions.

2.7 Permeability measurement

Permeability was measured with 40 kDa-FITC-dextran which is widely used as nanoparticles for paracellular transport experiments.[27,28] Fig. S3(a)† shows the injection of dextran into the blood vessel channel. The blood vessel channel functions as the substance donor, while the parathyroid channel, where dextran is delivered, serves as the substance acceptor. The detection line (indicated by the yellow line) with a length of 1800 μm, corresponding to the combined width of the two channels, was drawn. Fluorescence intensity along this line was measured using "Plot profile" of ImageJ, as shown in Fig. S3(b).† ΔC was the difference in average of fluorescence intensity between the substance donor and substance acceptor. dC/dx represents the gradient of the fluorescence intensity.

2.8 Measurement of secreted PTH

For measurement of PTH secretion, we collected the cellular supernatant. All collected culture medium was filtered using a 0.2 mm syringe filter and stored at −80 °C until measurement. Each culture medium was prepared in duplicate and analyzed for concentrations of secreted PTH by an electrochemical luminescence immune assay (ECLIA) using an Elecsys PTH kit (Roche, Germany).

3. Theory

3.1 Differentiation of TMSCs into parathyroid-like cells

The parathyroid gland is an endocrine organ mainly composed of chief cells.[29] It regulates calcium homeostasis by detecting low calcium levels and secreting parathyroid

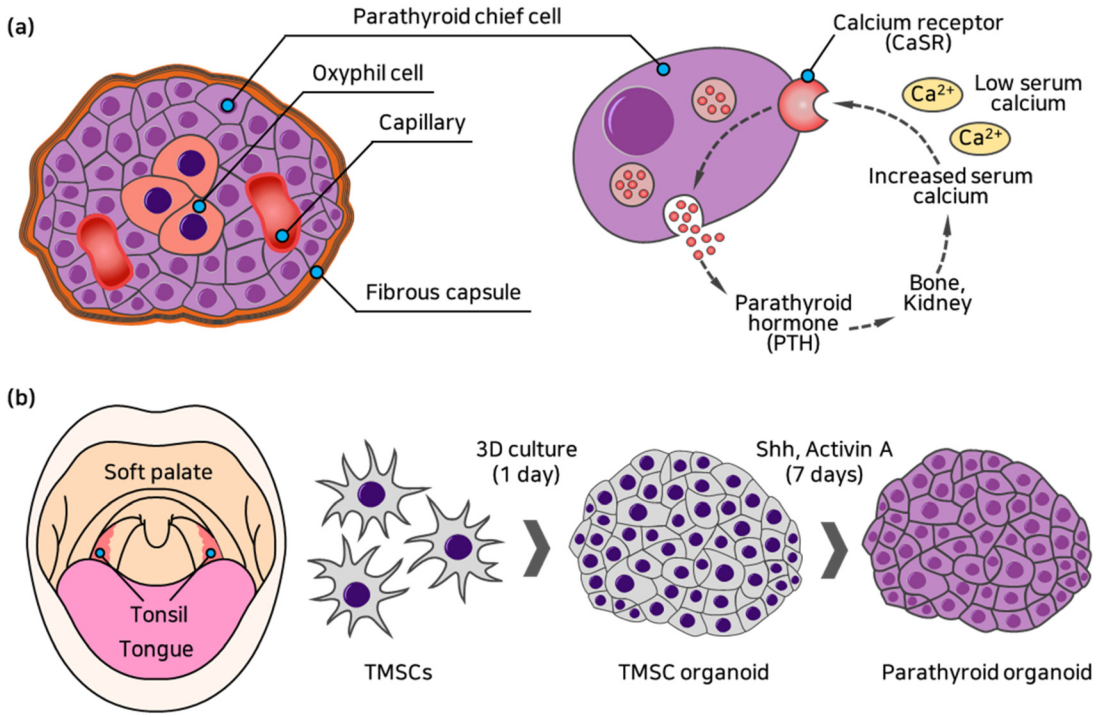

Fig. 1 (a) Illustration of parathyroid structure and calcium–parathyroid hormone interaction by a parathyroid chief cell. (b) Tonsil-derived MSCs and differentiation to parathyroid-like cells for the parathyroid organoid development.

hormone (PTH), as shown in Fig. 1(a).[30,31] Embryologically, parathyroid cells originate from the third pouch in the endoderm layer, and the expression of transcription factors in the pharyngeal endoderm is associated with the development of parathyroid precursors.[32] Tonsil tissue has its origin in the epithelial cells derived from the second pharyngeal pouch of the endoderm layer as well as lymphoid tissue derived from the mesoderm layer.[33] The relationship between the embryological development of the parathyroid and the intrinsic characteristics of tonsil tissue suggests that TMSCs can be easily differentiated into parathyroid phenotype as shown Fig. 1(b).

Soluble sonic hedgehog (Shh) and Activin A are generally used *in vitro* for stem cell differentiation into parathyroid cells.[19,34] Shh plays an important role in establishing precise domains of the parathyroid in the third pharyngeal pouch, and loss of Shh leads to the absence of dorsal parathyroid identity within the primordium.[35] Activin A is required for the functional maturation of various organ systems during the early stages of embryonic development and influences the differentiation of stem cells into definitive endoderm cells.[36] Indeed, the differentiation of stem cells into endodermal cells is influenced by various conditions related to Activin A, such as its concentration, culture conditions, application time, and interactions with different signaling pathways and differentiation factors.[37] Therefore, stem cells can be differentiated into parathyroid cells by employing suitable concentrations of differentiation factors (Shh, Activin A) and controlling the duration of the differentiation.

3.2 Permeability of vascular endothelium

Endocrine hormones transported through the bloodstream often need to pass through an endothelial barrier, and this transport across barriers can limit the rate of action and hormone concentration.[38] The vascular endothelium plays a crucial role in supplying nutrients to the underlying tissues and regulating vascular homeostasis, as well as maintaining barrier function.[39] Due to these important roles, the vascular endothelium is essential for the survival of organoids and the support of PTH secretion in response to calcium concentrations in the microenvironmental system. The permeability of the vascular endothelium refers to the tightness of intercellular junctions and regulates the transport of molecules. It can be calculated using Fick's first law as follows:[40]

$$P_{\mathrm{E}} = \frac{D}{\Delta C}\frac{\mathrm{d}C}{\mathrm{d}x} \quad (1)$$

where P_{E} is the permeability of vascular endothelium, ΔC is the difference in concentration between the substance donor and the substance acceptor, and $\mathrm{d}C/\mathrm{d}x$ is the gradient of concentration. The diffusion coefficient (D) is calculated using the Stokes–Einstein equation as follows:[41]

$$D = \frac{k_{\mathrm{B}}T}{6\pi\mu r} \quad (2)$$

where k_{B} is Boltzmann's constant, 1.3807×10^{-23} J K^{-1}, T is temperature (K), μ is the viscosity of culture medium, and r is the radius of molecules.

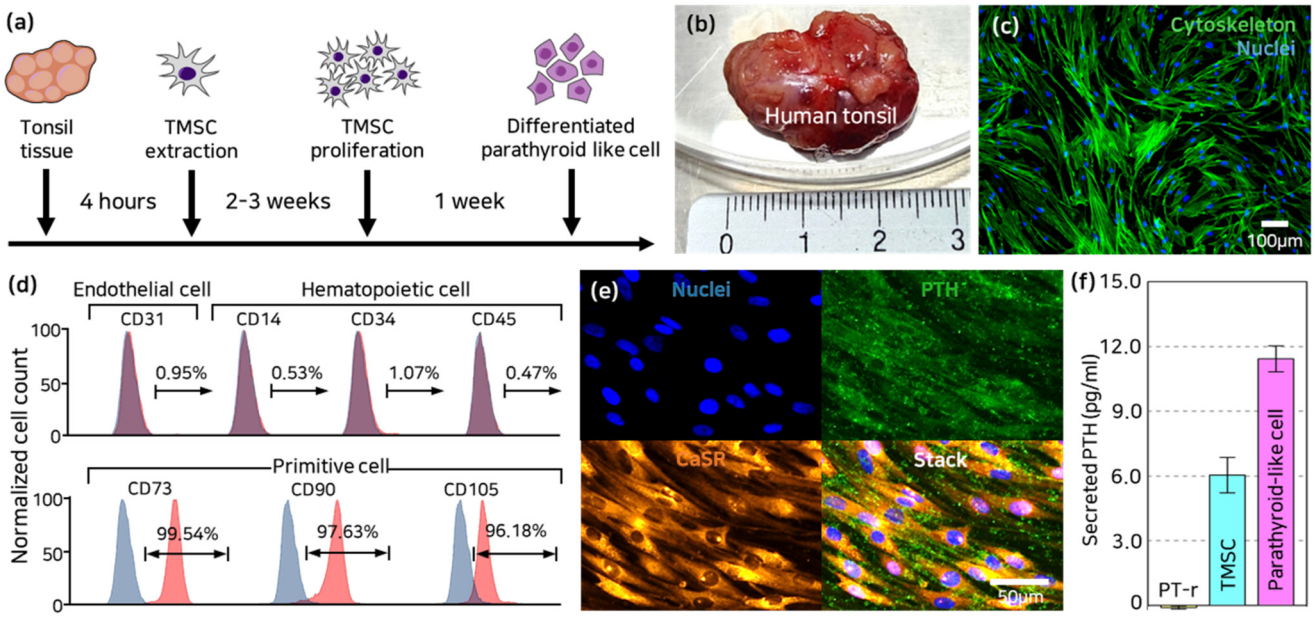

Fig. 2 (a) Procedure of parathyroid-like cells from human tonsil tissue by TMSC differentiation. (b) Human tonsil tissue and (c) proliferated TMSCs. Cytoskeleton (green) and nuclei (blue). (d) Fluorescence-activated cell sorter (FACS) analysis results to validate the TMSCs. (e) Differentiated from TMSCs into parathyroid-like cells. Nuclei (blue), PTH (green), and CaSR (orange). (f) PTH secretion by PT-r cells, TMSCs, and parathyroid-like cells, respectively.

4. Results and discussion

4.1 Differentiation into parathyroid-like cells

The differentiation protocol of TMSCs into parathyroid-like cells is shown in Fig. 2(a). We extracted TMSCs from the tonsil, as shown in Fig. 2(b), and proliferated them to ensure an adequate supply. Fig. 2(c) shows 3 weeks of proliferated TMSCs that were stained for cytoskeleton (green) and nuclei (blue) for morphological visualization. In the identification of cell subtypes, their primitive cell type clearly showed that the

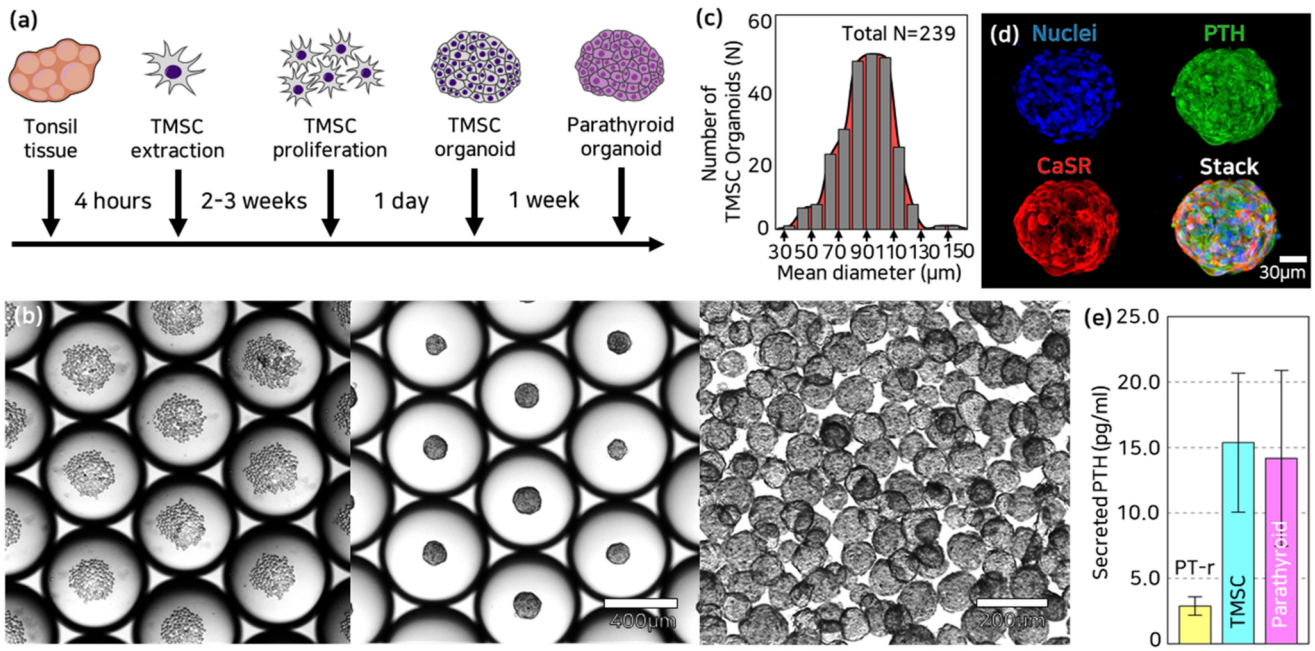

Fig. 3 (a) Procedure of parathyroid organoid development from human tonsil tissue by TMSC organoid differentiation. (b) Droplet-based 3D culture using TMSCs. (Left) TMSCs encapsulated in droplet, (middle) 1 day cultured and formed TMSC organoid in droplet, and (right) released TMSC organoid from droplets. (c) Size distribution of TMSC organoids (N = 239). (d) Differentiated TMSC organoid into parathyroid organoid. Nuclei (blue), PTH (green) and CaSR (deep red). (e) PTH secretion by organoids fabricated from the PT-r cell line, TMSC organoid, and parathyroid organoid, respectively.

proliferated TMSCs were not endothelial cells (CD31) or hematopoietic cells (CD14, CD34, CD45), but pure stem cells (CD73, CD90, CD105) as shown in Fig. 2(d). TMSCs were differentiated into parathyroid-like cells for 7 days, and the expression of PTH and calcium-sensing receptor (CaSR), which are the mature parathyroid functional components,[32] was clearly observed as shown in Fig. 2(e). The culture medium was analyzed to determine the secreted PTH. Parathyroid-like cells and TMSCs secreted 11.4 ± 0.8 pg ml^{-1} and 6.0 ± 0.6 pg ml^{-1} of PTH, respectively, and the PT-r cell line did not secrete PTH as shown in Fig. 2(f). Detailed information on the validation of PT-r cells is described in Fig. S4.†

4.2 Fabrication of parathyroid organoids

The parathyroid organoids were prepared following the procedure shown in Fig. 3(a), starting with the formation of TMSC organoids, which were subsequently differentiated into parathyroid organoids. TMSC organoids were formed using the droplet-based microfluidics system, which enables mass fabrication of organoids with uniform sizes Fig. 3(b) shows mass-fabricated TMSC organoids, while uniform-sized TMSC organoids with a diameter of 90.5 ± 9.5 μm were formed, as shown in Fig. 3(c). After TMSC organoids were differentiated into parathyroid organoids for 7 days using differentiation factors, they were validated using immunofluorescence staining. The expression of PTH and CaSR was well-developed as shown in Fig. 3(d). Parathyroid organoids, TMSC organoids, and PT-r organoids secreted 14.2 ± 6.7 pg ml^{-1}, 15.4 ± 5.3 pg ml^{-1}, and 2.9 ± 0.7 pg ml^{-1}, respectively as shown in Fig. 3(e). Parathyroid organoids and TMSC organoids secreted PTH at similar levels. There are two possible reasons for this phenomenon. The first reason is that stem cells, such as bone marrow stem cells, occasionally produce the PTH protein,[42] potentially enabling them to secrete PTH under specific conditions. The second reason is that under conditions of high cell density, PTH mRNA expression in parathyroid-like cells increases.[17] Maintaining a high cell density in a 3D cultured spheroid enhances intercellular communication, thereby inducing cell function.[43] Although both types of organoids secreted similar levels of PTH, it was important that parathyroid organoids secreted PTH within the range of normal serum PTH levels (10–65 pg ml^{-1}).[44,45]

4.3 Validation of parathyroid-on-a-chip

The parathyroid-on-chip consists of two separate compartments for the parathyroid microenvironment and the

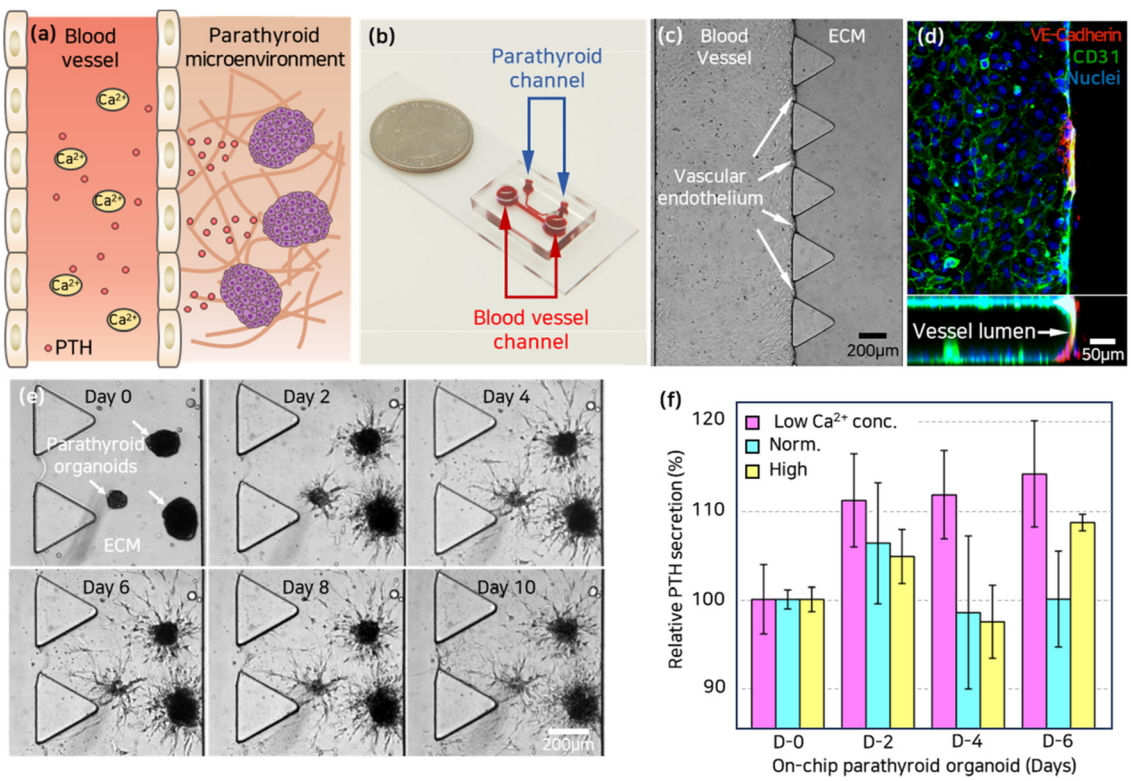

Fig. 4 (a) Illustration of parathyroid-on-a-chip which consists of a capillary blood vessel and parathyroid organoid. (b) Optical image of micro-fabricated parathyroid-on-a-chip. (c) Vascular endothelium in parathyroid-on-a-chip. (d) Vessel lumen of vascular endothelium. VE-cadherin (red), CD31 (green), and nuclei (blue). (e) Parathyroid organoid and vascular endothelium long-term co-culture in parathyroid-on-a-chip. (f) The secreted PTH with respective to the calcium level in the collected culture medium from the chip. Low (0.3 mM), normal (1.8 mM), and high (3.3 mM) $CaCl_2$ concentrations.

blood vessel as shown in Fig. 4(a and b), and they are connected by open windows between triangular pillars. HUVECs were cultured in the blood vessel channel as shown in Fig. 4(c). The vascular endothelium and its unique lumen structure are visible in Fig. 4(d), where VE-cadherin (red), CD31 (green), and nuclei (blue) are observed. The permeability of the vascular endothelium was calculated to be 2.41 ± 0.94 × 10^{-7} m s^{-1}, which falls within the normal range of capillary permeability, typically ranging from 1 to 4 × 10^{-7} m s^{-1}.[46] In the parathyroid channel, parathyroid organoid-laden fibrin gel was loaded and cultured as shown in Fig. 4(e), and the secretion of PTH was analyzed in the culture medium with different calcium conditions as shown in Fig. 4(f). The secreted PTH on the initial day was 22.7 ± 0.91 pg ml^{-1}, 25.2 ± 0.28 pg ml^{-1}, and 25.1 ± 0.35 pg ml^{-1} under low (0.3 mM), normal (1.8 mM), and high (3.3 mM) calcium conditions, respectively, all within the normal serum PTH range (15–65 pg ml^{-1}). To determine the relative increase in concentrations based on the period, the secreted PTH was normalized based on the initial day of secretion. On day 2, PTH secretion increased by 11.6 ± 5.5%, 6.6 ± 7.1%, and 5.0 ± 1.4% under low, normal, and high calcium conditions, respectively. On day 4, PTH secretion increased by 12.2 ± 5.2% under low calcium conditions and decreased by 1.5 ± 8.9% and 2.6 ± 3.1% under normal and high calcium conditions, respectively. After day 6, despite exhibiting the highest PTH secretion under low calcium conditions, PTH secretion was lower under normal calcium conditions compared to high calcium conditions. These results indicate that up to day 4, PTH secretion responds appropriately to the calcium concentration. Parathyroid-like cells secreted PTH at maximum levels on days 7 to 10 and subsequently decreased.[20] It suggests a weakening of the function of parathyroid-like cells (or parathyroid organoids) 10 days later. Therefore, we limit the expiration date of the parathyroid-on-a-chip to day 4 (11 days after differentiation), and it is deemed desirable to conduct candidate drug testing using this chip on days 2 to 4.

4.4 Engraftment by organoid branch extension

Vascularization is a crucial factor in guaranteeing the functionality of the transplanted organoids and successful engraftment in implantation therapies involving not only the parathyroid but also other organs. In the parathyroid-on-a-chip, the possibility of engraftment of parathyroid organoids was confirmed by measuring the branches of organoids because a vascular sprout indeed becomes a capillary.[47,48] The vascular endothelium was formed between the two separate compartments of the parathyroid-on-chip as shown in Fig. 5(a and b), and the parathyroid organoids were ladened in fibrin gel as shown in Fig. 5(c). The parathyroid

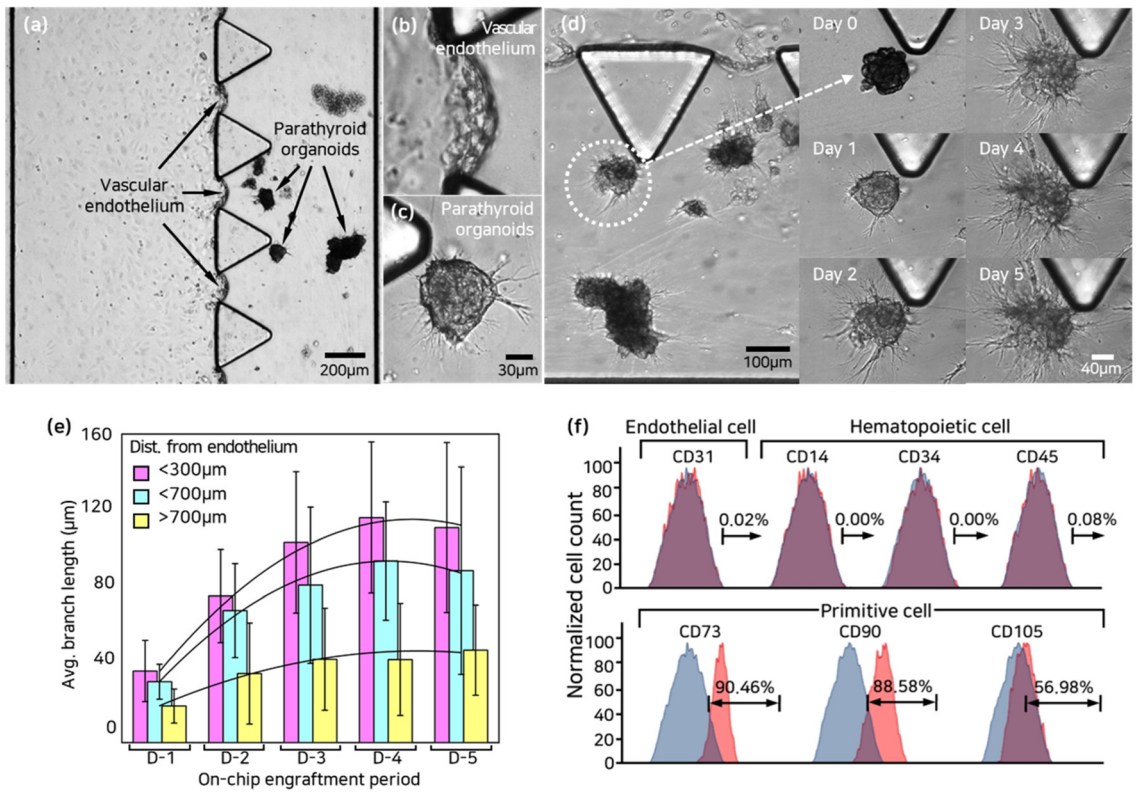

Fig. 5 (a and b) The vascular endothelium between the two separate compartments of the parathyroid-on-chip. (c) Parathyroid organoid-ladened ECM in parathyroid-on-a-chip. (d) The branch formation of parathyroid organoid over time. (e) The tendency of branch formation in relation to the distance from the vascular endothelium. (f) Fluorescence-activated cell sorter (FACS) analysis results to validate the parathyroid-like cell.

organoids formed branches over time as shown in Fig. 5(d). Parathyroid organoids located within 300 μm, between 300 and 700 μm, and more than 700 μm of the vascular endothelium formed branch lengths of 37.1 ± 15.9 μm, 31.5 ± 9.1 μm, 18.9 ± 8.8 μm after 1 day, respectively. After 4 days, those within 300 μm and between 300 and 700 μm reached peak branch lengths of 116.7 ± 39.2 μm, 94.1 ± 30.7 μm, respectively, and no further increase in branch length was observed. Parathyroid organoids located at more than 700 μm reached peak branch lengths of 47.9 ± 23.4 μm after 5 days. There was a clear trend of forming longer branches as the parathyroid organoids approached the vascular endothelium as shown in Fig. 5(e). These results suggest that it is favorable to have proximity to blood vessels as a nutrient source for successful engraftment of parathyroid organoids. To investigate the reason for branch formation, differentiated parathyroid-like cells were analyzed using fluorescence-activated cell sorting. They still possessed the characteristics of stem cells as shown in Fig. 5(f). In particular, branch formation could be due to the expression of CD105, which is associated with angiogenesis and development, and in maintaining vessel wall integrity.[49]

5. Conclusions

In this study, we developed a parathyroid-on-a-chip capable of simulating the interaction between the parathyroid and blood vessels. This chip can be utilized to validate the efficacy of candidate drugs by injecting them into the blood vessel channel and analyzing the affected PTH secretion. Cinacalcet HCl is a substance used for the treatment of hyperparathyroidism by increasing the sensitivity of CaSR and subsequently reducing PTH secretion.[50] In the next study, we plan to evaluate the drug delivery effectiveness of parathyroid-on-a-chip using cinacalcet HCl. However, candidate drugs for hypoparathyroidism have not yet been identified, and we are actively searching for them. This underscores the urgency of research and development for new drugs aimed at restoring parathyroid functionality. Parathyroid-on-a-chip is expected to invigorate the pharmaceutical industry focus on parathyroid.

Another key point of this study is that it used normal human-derived cells. Cell lines,[1,2,51,52] patient-derived parathyroid cells,[34,53] and animal-derived cells[54] have been used in parathyroid research, but these approaches may have limitations in representing human normal parathyroid cells. As shown in Fig. S4, S5, and Table S1,† it is indeed the case that both the cell line and primary cells lost their parathyroid function or faced difficulties in obtaining a sufficient supply. Human TMSCs can differentiate into parathyroid-like cells with parathyroid function,[20] which is advantageous for ensuring an adequate number of parathyroid cells and overcoming species or cellular differences. Therefore, parathyroid-on-a-chip, composed of human-derived cells, is suitable for complementing animal experiments in testing candidate drugs.

Author contributions

Sunghan Lee: data curation, methodology, roles/writing – original draft, validation, visualization, investigation. Hyo-Il Jung: writing – review & editing, supervision. Jaehun Lee: data curation, visualization. Youngwon Kim: methodology, validation. Jaewoo Chung: data curation, methodology. Han Su Kim: investigation. Ji Seok Lim: funding acquisition, investigation. Ki Chang Nam: investigation. Yun-Sung Lim: conceptualization, methodology, investigation, writing – review & editing. Han Seok Choi: conceptualization, funding acquisition, investigation, writing – review & editing. Bong Seop Kwak: conceptualization, funding acquisition, investigation, writing – review & editing, visualization, supervision.

Conflicts of interest

The authors declare no conflict of interest.

Acknowledgements

This study was supported by the National Research Foundation of Korea (NRF) grant funded by the Korean Government (MEST) (NRF-2022R1A2C2003103, NRF-2021R1A2C3011254, and NRF-2020R1A5A1018052) and Ministry of Education (NRF-2018R1D1A1A02086061).

References

1 S. Fabbri, S. Ciuffi, V. Nardone, A. R. Gomes, C. Mavilia, R. Zonefrati, G. Galli, E. Luzi, A. Tanini and M. L. Brandi, *Endocrine*, 2014, **47**, 90–99.
2 M. Kawahara, Y. Iwasaki, K. Sakaguchi, T. Taguchi, M. Nishiyama, T. Nigawara, M. Kambayashi, T. Sawada, X. Jing, M. Miyajima, Y. Terada, K. Hashimoto and T. Suda, *Bone*, 2010, **47**, 534–541.
3 M. J. Horwitz and A. F. Stewart, *J. Clin. Endocrinol. Metab.*, 2008, **93**, 3307–3309.
4 J. Bollerslev, L. Rejnmark, C. Marcocci, D. M. Shoback, A. Sitges-Serra, W. van Biesen and O. M. Dekkers, *Eur. J. Endocrinol.*, 2015, **173**, G1–G20.
5 X. Chen, J. Sun and X. Li, *Med. Hypotheses*, 2021, **149**, 2020–2022.
6 T. Lu, B. Yang, R. Wang and C. Qin, *Front. Immunol.*, 2020, **10**, 3060.
7 R. Driver and S. Mishra, *BioChip J.*, 2023, **17**, 1–23.
8 S. Stucker, J. De Angelis and A. P. Kusumbe, *Front. Physiol.*, 2021, **12**, 624928.
9 C. Ma, Y. Peng, H. Li and W. Chen, *Trends Pharmacol. Sci.*, 2021, **42**, 119–133.
10 J. Han, U. Kang, E. Y. Moon, H. Yoo and B. Gweon, *BioChip J.*, 2022, **16**, 255–269.
11 M. Jang and H. N. Kim, *BioChip J.*, 2023, **17**, 133–146.
12 A. Agarwal, J. A. Goss, A. Cho, M. L. McCain and K. K. Parker, *Lab Chip*, 2013, **13**, 3599–3608.
13 M. Humayun, C.-W. Chow and E. W. K. Young, *Lab Chip*, 2018, **18**, 1298–1309.

14 S. Mao, D. Gao, W. Liu, H. Wei and J.-M. Lin, *Lab Chip*, 2012, **12**, 219–226.
15 D. Gao, H. Liu, J.-M. Lin, Y. Wang and Y. Jiang, *Lab Chip*, 2013, **13**, 978–985.
16 K.-J. Jang, A. P. Mehr, G. A. Hamilton, L. A. McPartlin, S. Chung, K.-Y. Suh and D. E. Ingber, *Integr. Biol.*, 2013, **5**, 1119–1129.
17 J. Y. Kim, S. Park, S.-Y. Oh, Y. H. Nam, Y. M. Choi, Y. Choi, H. Y. Kim, S. Y. Jung, H. S. Kim, I. Jo and S.-C. Jung, *Int. J. Mol. Sci.*, 2022, **23**, 715.
18 Y. S. Park, J. Y. Hwang, Y. Jun, Y. M. Jin, G. Kim, H. Y. Kim, H. S. Kim, S. H. Lee and I. Jo, *Acta Biomater.*, 2016, **35**, 215–227.
19 K. H. Ryu, K. A. Cho, H. S. Park, J. Y. Kim, S. Y. Woo, I. Jo, Y. H. Choi, Y. M. Park, S. C. Jung, S. M. Chung, B. O. Choi and H. S. Kim, *Cytotherapy*, 2012, **14**, 1193–1202.
20 Y. S. Park, H. S. Kim, Y. M. Jin, Y. Yu, H. Y. Kim, H. S. Park, S. C. Jung, K. H. Han, Y. J. Park, K. H. Ryu and I. Jo, *Biomaterials*, 2015, **65**, 140–152.
21 B. Kwak, Y. Lee, J. Lee, S. Lee and J. Lim, *J. Controlled Release*, 2018, **275**, 201–207.
22 E. L. Bingham, S. P. Cheng, K. M. Woods Ignatoski and G. M. Doherty, *Stem Cells Dev.*, 2009, **18**, 1071–1080.
23 Y. Liu, J. Li, J. Zhou, X. Liu, H. Li, Y. Lu, B. Lin, X. Li and T. Liu, *Micromachines*, 2022, **13**, 225.
24 J. Kim, M. Chung, S. Kim, D. H. Jo, J. H. Kim and N. L. Jeon, *PLoS One*, 2015, **10**, e0133880.
25 F. Pisapia, W. Balachandran and M. Rasekh, *Appl. Sci.*, 2022, 12.
26 M. Kang, W. Park, S. Na, S.-M. Paik, H. Lee, J. W. Park, H.-Y. Kim and N. L. Jeon, *Small*, 2015, **11**, 2789–2797.
27 A. Thomas, S. Wang, S. Sohrabi, C. Orr, R. He, W. Shi and Y. Liu, *Biomicrofluidics*, 2017, **11**, 1–17.
28 M. R. Dreher, W. Liu, C. R. Michelich, M. W. Dewhirst, F. Yuan and A. Chilkoti, *J. Natl. Cancer Inst.*, 2006, **98**, 335–344.
29 S. N. Parlak, *Anatolian Journal of Biology*, 2022, **3**, 11–13.
30 D. Goltzman, *Endocrinol. Metab. Clin. North Am.*, 2018, **47**, 743–758.
31 K. Peissig, B. G. Condie and N. R. Manley, *Endocrinol. Metab. Clin. North Am.*, 2018, **47**, 733–742.
32 E. L. Bingham, S. P. Cheng, K. M. W. Ignatoski and G. M. Doherty, *Stem Cells Dev.*, 2009, **18**, 1071–1080.
33 K. A. Cho, H. J. Lee, H. Jeong, M. Kim, S. Y. Jung, H. S. Park, K. H. Ryu, S. J. Lee, B. Jeong, H. Lee and H. S. Kim, *World J. Stem Cells*, 2019, **11**, 506–518.
34 M. E. Noltes, L. H. J. Sondorp, L. Kracht, I. F. Antunes, R. Wardenaar, W. Kelder, A. Kemper, W. Szymanski, W. T. Zandee, L. Jansen, A. H. Brouwers, R. P. Coppes and S. Kruijff, *Stem Cell Rep.*, 2022, **17**, 2518–2530.
35 B. A. Moore-Scott and N. R. Manley, *Dev. Biol.*, 2005, **278**, 323–335.
36 L. Andreasson, H. Evenbratt, R. Mobini and S. Simonsson, *J. Biotechnol.*, 2021, **325**, 173–178.
37 S. Sulzbacher, I. S. Schroeder, T. T. Truong and A. M. Wobus, *Stem Cell Rev. Rep.*, 2009, **5**, 159–173.
38 C. M. Kolka and R. N. Bergman, *Physiology*, 2012, **27**, 237–247.
39 J. E. Deanfield, J. P. Halcox and T. J. Rabelink, *Circulation*, 2007, **115**, 1285–1295.
40 B. Chung, J. Kim, H.-W. Liu, J. Nam, H. Kim, H. J. Oh, Y. H. Kim and S. Chung, *Micro and Nano Syst. Lett.*, 2019, **7**, DOI: **10.1186/s40486-019-0092-7**.
41 S. Ramanujan, A. Pluen, T. D. McKee, E. B. Brown, Y. Boucher and R. K. Jain, *Biophys. J.*, 2002, **83**, 1650–1660.
42 W. Zou, B. Yang, L. Wu, T. Chen, D. Zhang, M. Xiong, J. Chen and T. Zou, *Blood*, 2011, **118**, 4817.
43 Y. H. Jung, K. Park, M. Kim, H. Oh, D. H. Choi, J. Ahn, S. B. Lee, K. Na, B. S. Min, J. A. Kim and S. Chung, *BioChip J.*, 2023, DOI: **10.1007/s13206-023-00099-y**.
44 R. Promberger, J. Ott, F. Kober, M. Karik, M. Freissmuth and M. Hermann, *Thyroid*, 2011, **21**, 145–150.
45 C. Mischis-Troussard, P. Goudet, B. Verges, P. Cougard, C. Tavernier and J. F. Maillefert, *QJM*, 2000, **93**, 365–367.
46 Y. Kim, J. Lee, S. Lee, H.-I. Jung and B. Kwak, *Biosens. Bioelectron.*, 2024, **243**, 115787.
47 P. Kannan, M. Schain and D. P. Lane, *Front. Pharmacol.*, 2022, **13**, 883083.
48 S. Wang, L. Mundada, S. Johnson, J. Wong, R. Witt, R. G. Ohye and M.-S. Si, *Stem Cells Transl. Med.*, 2015, **4**, 339–350.
49 E. Fonsatti and M. Maio, *J. Transl. Med.*, 2004, **2**, 1–7.
50 J. A. Barman Balfour and L. J. Scott, *Drugs*, 2005, **65**, 271–281.
51 K. Sakaguchi, K. Ikeda, F. Curcio, G. D. Aurbach and M. L. Brandi, *J. Bone Miner. Res.*, 1990, **5**, 863–869.
52 K. Sakaguchi, A. Santora, M. Zimering, F. Curcio, G. D. Aurbach and M. L. Brandi, *Proc. Natl. Acad. Sci. U. S. A.*, 1987, **84**, 3269–3273.
53 P. Sethu, T. A. Haglund, A. J. Rogers, H. Chen, J. Porterfield and C. J. Balentine, *Cells Tissues Organs*, 2019, **206**, 54–61.
54 P. Zhang, H. Zhang, W. Dong, Z. Wang, Y. Qin, C. Wu and Q. Dong, *Int. J. Endocrinol.*, 2020, **2020**, 1860842.